A Miniaturized Wearable Two-port Loop Rectenna for Energy Harvesting at millimeter wave

Published Version:
Augello, E., Fazzini, E., Benassi, F., Masotti, D., Costanzo, A. (2023). A Miniaturized Wearable Two-port Loop Rectenna for Energy Harvesting at millimeter wave. NEW YORK, USA : IEEE [10.1109/WPTCE56855.2023.10216094].

Availability:
This version is available at: https://hdl.handle.net/11585/943156 since: 2023-09-27

Published:
DOI: http://doi.org/10.1109/WPTCE56855.2023.10216094

E. Augello, E. Fazzini, F. Benassi, D. Masotti and A. Costanzo

A Miniaturized Wearable Two-port Loop Rectenna for Energy Harvesting at millimeter wave

In: 2023 IEEE Wireless Power Technology Conference and Expo (WPTCE), San Diego, CA, USA, 2023, pp. 1-6

A Miniaturized Wearable Two-port Loop Rectenna for Energy Harvesting at millimeter wave

1st Elisa Augello
DEI "Guglielmo Marconi"
University of Bologna
Bologna, Italy
elisa.augello2@unibo.it

2nd Enrico Fazzini
DEI "Guglielmo Marconi"
University of Bologna
Bologna, Italy
enrico.fazzini@unibo.it

3rd Francesca Benassi
DEI "Guglielmo Marconi"
University of Bologna
Bologna, Italy
francesca.benassi9@unibo.it

4th Diego Masotti
DEI "Guglielmo Marconi"
University of Bologna
Bologna, Italy
diego.masotti@unibo.it

5th Alessandra Costanzo
DEI "Guglielmo Marconi"
University of Bologna
Cesena, Italy
alessandra.costanzo@unibo.it

***Abstract*—The design of a novel two-port loop antenna, operating in the 30-GHz band, is proposed as the energy receiver in a mm-wave WPT link, exploiting Bessel beam launchers for power transmission. For wearable applications this solution allows to combine the focusing capabilities of the launchers with miniaturization, important requirements for wearable devices. Starting from a rectangular loop length chosen to cover the main beam area, its geometry is outfitted with meandered sections of conductors that act as phase shifters, to ensure uniformity of field distribution and getting rid of field nulls. To further enhance field uniformity, two differential ports, placed in symmetrical positions, are selected and the energy transfer capabilities of the wireless link, consisting of the launcher and the modified loop, are computed by numerical simulations for several distances, both in air and in proximity of human tissues. Two identical differential rectifiers, adopting mm-wave GaAs Schottky diodes, are designed with the proposed two-port loop as the feeding network. An RF-to-dc efficiency of 30 % is predicted for an RF power of 10 dBm at 31.67 GHz. The proposed system can be a feasible solution to be used in compact WPT applications, particularly when wearability, compactness, and lightness are required.**

***Index Terms*—WPT, mm-wave, loop, wearable.**

I. Introduction

In recent years, wireless power transfer (WPT) has become an increasingly active area of research, particularly at millimeter-wave frequencies. One promising approach for mm-wave WPT is the use of loop antennas as receivers, as one of the best compromise between compactness and overall efficiency. In particular, WPT systems that use loop antennas operating at millimeter wave frequencies have shown to be promising for applications such as Internet of Things (IoT) devices [1], medical implants, and wearables [2], thanks to their reduced dimensions [3]. These systems take advantage of the benefits of high-frequency electromagnetic waves, such as reduced signal interference, increased spatial resolution, and the ability to transmit data and power at the same time. This work proposes the design and performance analysis of a 31.67 GHz loop antenna to be applied in wearable wireless power transfer applications, introducing a design that boasts miniaturization and compactness, aiming to be a valuable option for radiative near field links made of Bessel Beam launchers [4].

This type of launchers shows noticeable properties when used for the transmitting side thanks to their diffraction-free nature and their focusing capabilities [5], placing themselves as an alternative to already established focusing techniques, such as Time Modulated Arrays (TMA) [6], which are mainly focused on longer distances. In the context of wearable devices, however, their use as receiver shows some limitations for multiple reasons. The rigid structure coming from the metallic nature of the waveguide does not allow to think of bendable solutions or different shapes that could adapt better to human tissues. Their non-diffractive range is strictly related to their dimensions, making challenging to have high level of miniaturization for a fixed frequency of operation, unless a reduction of the application range is accepted.

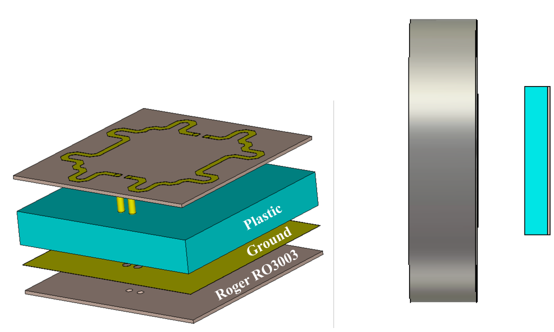

(a) (b)

Fig. 1. (a) Stack-up of the proposed wearable 30 GHz loop and (b) side view of the loop in front of to a Bessel Beam launcher operating at the same frequency.

Furthermore, the wireless power transfer link presented in [4] accounts for the use of two TE-polarized Bessel Beam launchers, both in transmission and reception. Although performance are promising, the only drawback lies in the overall geometry of the launcher, which indeed allow for an electrical decoupling with the surface it is laid on, but at the expense of a resonant cavity having a 3-cm diameter and 7-mm thickness. Therefore, the aim of this article is to describe a possible design of a suitable receiver to be used inside a WPT link having a Bessel Beam launcher only as transmitter. The challenge is finding a layout that would boast a higher level of miniaturization while remaining efficient in terms of wireless power transfer capabilities.

Figure 1a shows a pictorial representation of the proposed stack-up for the receiver side of the WPT link and Fig 1b compares the form factors of the two sub-systems. The overall volume of the proposed system is $15\times15\times3$ mm^3. As can be noticed, the suggested design introduces an improvement not only in the miniaturization factor along the transversal direction, leading to a reduction of about 50 % in the diameter, but in particular on the overall thickness of the structure, with a reduction of around 57 %, together with the possibility of realizing it completely flexible. The TE-polarized Bessel Beam launcher used for comparison, has been designed and thoroughly described in [4]. The work is organized as follows: Section II describes the operative steps of the loop antenna design, in Section III a link budget estimation is carried out and performance are compared with state-of-the-art radiative near field WPT solutions, Section IV presents the design and optimization of a balanced rectifier, and finally, conclusions are drawn in Section V.

II. Engineered design of the mm-wave loop

Due to the electromagnetic nature of the chosen loop, the field distribution along the longitudinal direction, as well as the complex power associated to it, is mainly due to the magnetic field component. In particular, a suitable transmitter must be chosen to transmit a complex EM power to be mainly proportional to the $|H_z|$ component of the generated electromagnetic field; thus a transmitter exciting a TE-mode must be selected, such as a TE-polarized Bessel Beam Launcher designed in [4]. Conventional loop antennas for WPT are of the "electrically small" type (i.e. perimeter smaller than half the operating wavelength) to produce a strong magnetic field in the central area. However, for the present case, the loop is much longer, due to the mm-wave operating frequency of the Bessel Beam Launcher used in transmission, which is approximately 30 GHz. When electrically small loop antennas operate at mm-wave, the corresponding perimeter is of few millimeters, resulting in a challenging realization and an extremely reduced interrogation zone. In this context, the receiving loop antenna has been designed with the main aim of maximizing the compactness and reducing the overall encumbrance when applied in a wearable context. For this reason, the loop length is chosen in such a way that the enclosed area corresponds to the cross section of the main Bessel beam for distances belonging to its non-diffractive range, as depicted Fig. 2.

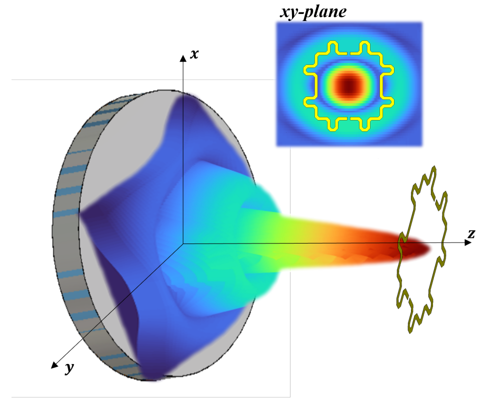

Fig. 2. Pictorial representation of the wireless power transfer link highlighting the relation between the loop dimension and the main beam of the launcher for a general case.

This way, having the majority of the power transferred by the Bessel transmitter concentrated in the main beam, allows for the loop to harvest a consistent amount of power while halving the overall dimensions both in the longitudinal and transversal direction. Moreover, it is worth noticing that the proposed loop layout can be easily realized on flexible materials, whereas the Bessel Beam cavity requires a more rigid structure, thus promising improvements are not only size-related but also on the wearability of the device itself. An initial design accounts for a single-loop squared layout which fulfils the previously-mentioned requirements. The current, flowing through the perimeter, experiences a phase inversion after every $\lambda_0/2$ travelled length, which results in current nulls. Considering a simple square loop, fed by one port, and having a side length of 10 mm, from Fig. 3a, it can be inferred that the current shows eight different amplitude nulls.

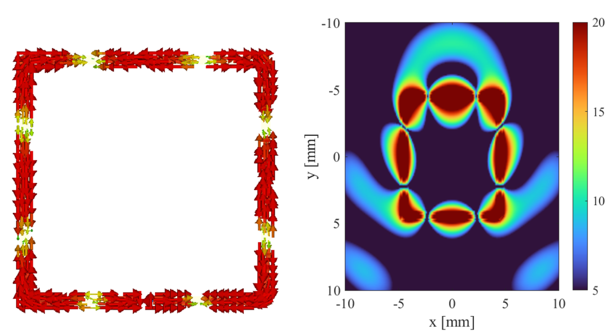

(a) (b)

Fig. 3. (a) Current and (b) magnetic field distribution (dB (A/m)) for the loop fed with a single port.

The corresponding magnetic field intensity, displayed in Fig. 3b, shows weaker levels in the central area with respect to the proximity of the loop metallization. For the present case, the receiver is realized on a Rogers RO3003 ($\varepsilon_r = 3$,

$\tan\delta = 0.001$) having a thickness of 0.254 mm. In order to overcome this lack of uniform field distribution, the layout is modified introducing meandered portions of the conductor with proper length to act as phase shifters, see Fig. 4 for reference, similar to what has been realized in [7].

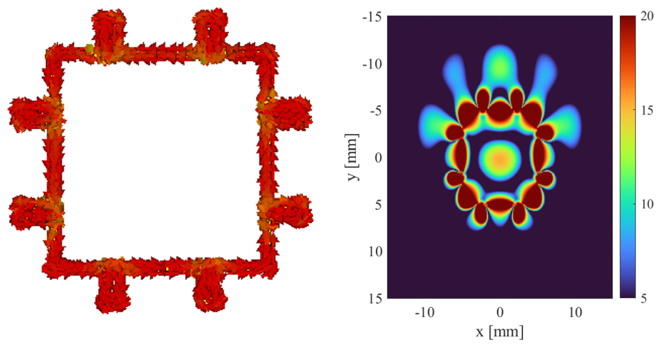

(a) (b)

Fig. 4. (a) Current and (b) magnetic field distribution (dB (A/m)) for the loop, modified with phase shifters, fed with a single port.

Phase shifters allow to compensate for each point of minimum, ensuring uniform current along the loop sides. Each phase shifter has a length of $\lambda_0/2$, which corresponds to the distance between two subsequent zeros of the surface current. In this way, a more uniform magnetic field distribution is obtained inside the loop perimeter together with a strong component located in the centre of the loop, directed along the longitudinal direction z. The introduction of the phase shifters enlarges the total loop length of the structure from $4\lambda_0$ to $8\lambda_0$, and a fine tuning of the shifters position and length is required, especially considering the operating frequency involved. However, this optimized layout shows an asymmetrical behaviour of the field distribution, due to the feeding section located at the bottom of the loop. It can be observed that, in correspondence of the port location, a portion of magnetic field is generated outside the central area.

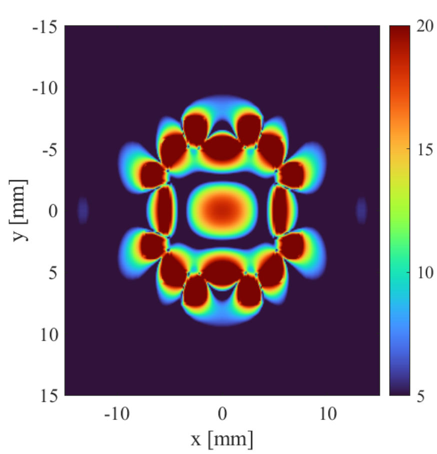

Fig. 5. Magnetic field distribution (dB (A/m))for the loop, modified with phase shifters, fed with balanced ports.

At such high operating frequency the presence of the port introduces a discontinuity which creates an unbalance distribution of the electromagnetic field. For this reason, a second feeding port has been located diametrically opposite to the first one in such a way that the discontinuity effect is balanced and, consequently, the generated field. Each port is phased coherently to ensure a uniform current distribution along the loop. This two-port arrangement will be fed with one half of the power per each port with respect to the single-feed case, in order to ensure a proper comparison. As can be inferred from Fig. 5, the magnetic field distribution shows higher intensity and uniformity in the central area, avoiding field dispersion in the adjacent regions. Moreover, the corners of each meandered section have been trimmed to be in compliance with the high operating frequency, and minimize unwanted radiations and power losses, as shown in Fig. 6a.

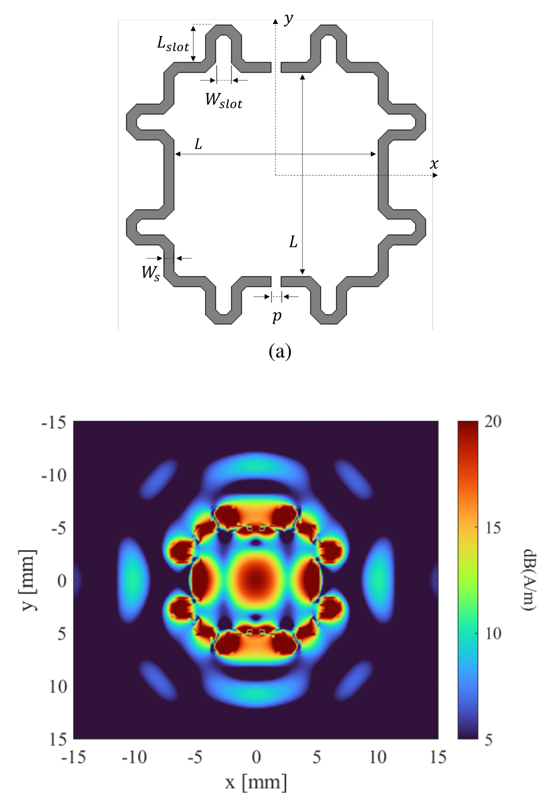

(b)

Fig. 6. (a) Schematic representation of the proposed 30 GHz loop: $L_{slot} = 1.8\ mm$, $W_{slot} = 0.8\ mm$, $L = 9.7\ mm$, $W_s = 0.5\ mm$, $p = 0.5\ mm$, (b) magnetic field distribution (dB (A/m)) for the multilayer structure of the engineered loop, placed on a skin layer.

Given the operative context, after validating the loop performance in air by means of full-wave simulations, the system is finely tuned accounting for the presence of a layered structure in which biological tissues must be modelled accordingly. In particular, a thin layer of plastic is interposed between the loop and the ground plane. The thickness of the plastic layer, ($\varepsilon_r = 2.5$, $\tan\delta = 0.018$ @30 GHz), has been chosen in order to be able to position the ground plane layer at the reference distance of $\lambda_0/4$, which allows it to act as a reflector to ensure maximization of the magnetic field towards the broadside direction, without affecting negatively the correct functioning of the loop. The presence of biological tissues is accounted for by introducing a skin layer ($\varepsilon_r = 14.4$, $\tan\delta = 1.08$ @30 GHz) of 2 mm thickness on top of which the whole structure is positioned and simulated. A schematic representation of the proposed stack-up is shown in Fig. 1 (a). The system accounts for the presence of four via holes that connect the loop to its dedicated circuitry located on the bottom layer. Having introduced such multilayered structure, as well as the via holes, implies a fine tuning of the loop geometry, whose final parameters are reported in Fig. 6a. As can be inferred by the field distribution in Fig. 6b, the introduction of a ground plane offers a proper isolation from the skin layer resulting in a generated magnetic field distribution that is not strongly affected by the presence of the body surface.

III. Link Budget Estimation of the mixed WPT link

In order to estimate the received power range, to conveniently design and optimize the rectifier, a link power budget has been computed. Moreover, the designed loop aims at boasting reduced dimensions but with sufficiently efficient performance in terms of wireless power transfer, when compared with a link adopting Bessel Beam launchers on both the receivers and the transmitter sides [4]. For this reason, the performance are evaluated for mixed links: the first one uses a TE-polarized Bessel Beam launcher, modelled according to [4], as transmitter and the designed loop as receiver while performing the analysis in air, whereas the second link accounts for the presence of the skin layer. The simulation accounting for the dielectric slab is of a paramount importance to mimic the situation in which the loop antenna is worn. As expected, the presence of the skin layer introduces degradation on the received power level, however, the overall dimensions, reduced of about 50 % with respect to the equivalent link exploiting two Bessel Beam launchers, allow to make this implemented design a valid solution for a lighter, miniaturized and thinner wearable receiver. Given the reduced operative distances between the transmitter and the receiver, the far-field approximation does not hold, thus the Friis equation cannot be used for the computation of the link power budget.

TABLE I
Received power levels

Distance $[mm]$	[4] [dBm]	**Proposed receiver in air [dBm]**	**Proposed receiver at 2.5 mm from skin [dBm]**
20 mm	15.8	13.9	11.6
30 mm	9.2	8.9	5.1
40 mm	4.9	4	-2

A way to perform this calculation, valid for any possible operative zone, is the method described in [8], which allows to rigorously and efficiently compute the received power of a wireless link for different TX-RX distances. The received power is evaluated considering a 27 dBm transmitted power and increasing separation distances between the transmitter and the receiver equal to 20, 30 and 40 mm, respectively, and the obtained values are listed in Tab.I.

Given the wearable context, the compliance with the guidelines for exposure to electromagnetic fields must be evaluated. The Specific Absorption Rate (SAR) has been calculated considering the maximum value of received power (11.6 dBm) at each balance port. The maximum obtained value is 0.0048 W/Kg, averaged of 10 g of tissue, allowing this system to operate below the safety limits that, for the operating frequency, are of 2 W/Kg.

IV. Balanced rectifier design

In this work, to be in compliance with the loop layout, a differential rectifier is implemented. Multiple kinds of differential rectifiers are reported in literature, as in [9]–[11]. Their use in energy harvesting applications is extensively validated (see [12], [13]) and motivated from the fact that antennas with differential feeding usually provide a high level of efficiency. In [14], a differential rectifier is exploited with a rectenna design, avoiding the use of via-holes connection in favour of a more practical and easy-to-be-realized system. A schematic representation of the proposed layout is depicted in Fig.7.

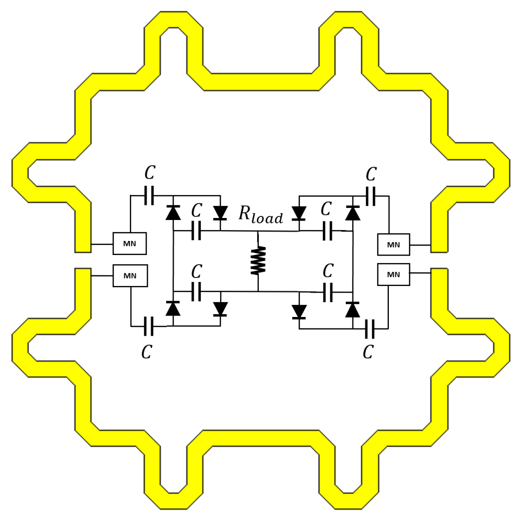

Fig. 7. Schematic representation of the proposed loop embedding the balanced rectifier $C = 50\ pF$, $R_{load} = 5000\ \Omega$. The circuitry, hosted in the bottom layer, is schematically represented for reference purposes.

The presence of two balanced ports, introduced to improve the field distribution, requires the use of a four-branch rectifier topology, schematically depicted in Fig. 7. As previously discussed in Section II, the presence of a ground plane located at $\lambda_0/4$ has the main function of acting as a reflector, enhancing the magnetic field density in the centre of the loop along the broadside direction, while also ensuring an electrical decoupling with the body surface. This layout can be exploited to design the rectifier circuitry on the bottom layer, removing the influence that physical components may introduced when located coplanar to the loop. For this reason, the loop is connected to the input of the matching network on the bottom layer by means of four 0.3-mm diameter via holes. The four via holes must be taken into account when designing and optimizing the circuitry. To carry out this, their equivalent inductance can be modelled, as described in [15], and the obtained values are placed in the linear subnetwork of the rectifier circuit. Each branch consists of a matching network (MN in Fig. 7), followed by a capacitor $C = 50\ pF$ used as a DC-block. The differential rectifier is based on four voltage-doubler stages, two for each balanced port, made of Macom MA4E2037 diodes, chosen for their low junction capacitance ($20\ fF$). The rectifier has been optimized to maximize the $\eta_{RF-to-dc}$ power conversion efficiency within a received power range that is in compliance with the received power level calculated in Tab.I when the skin layer is present. The predicted performance, plotted in Fig. 8, shows an $\eta_{RF-to-dc}$ that has a maximum value of 28% at $20\ mm$ distance between the TE-polarized Bessel Beam launcher and the designed loop. These obtained performance, despite being satisfying, suffer from the increased number of diodes with respect to the rectifier layout used in [4], resulting in extra losses at mm-waves.

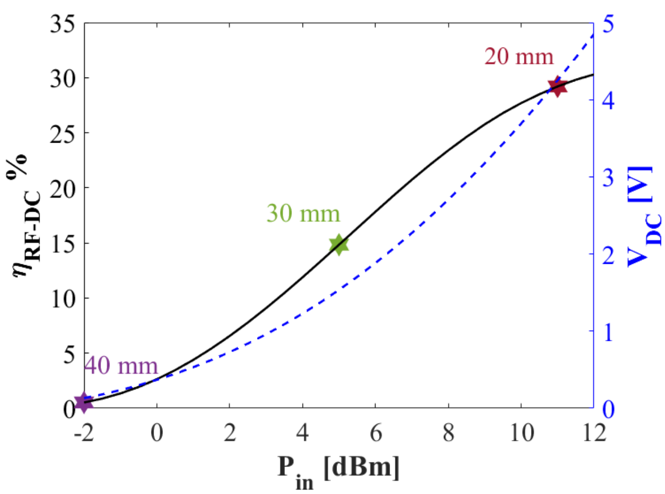

Fig. 8. $\eta_{RF-to-dc}$ power conversion efficiency vs dc-voltage levels for different received power levels.

However, the obtained results are aligned with the current state-of-the-art for the mm-wave rectenna, leading this solution to be a valid option to perform efficient wireless power transfer while achieving miniaturization, lightness and, in a possible future development, flexibility. Due to the high operating frequency and the multilayer design, the fabrication process will be matter of future research activities.

V. Conclusion

The design of a novel, mm-wave loop antenna for wearable wireless power transfer applications has been introduced in this work. Field distribution uniformity has been achieved by introducing proper meandered conductor sectors, acting as phase shifters, eliminating the periodic occurrence of current nulls. Furthermore, two differential ports have been suitably located in symmetric positions to be connected to a balanced network of rectifiers. The design steps (and the chosen operating frequency) have aimed for miniaturization and compactness in comparison to available solutions based on wireless links adopting radiative near field structures. The evaluation of the wireless link budget, using a numerical method, enables the optimization of a balanced rectifier, whose results are consistent with the literature. To be fully compliant with the wearability requirements, simulations of the entire system have been performed, accounting for the presence of biological tissue layers showing promising results and making the presented system a viable option in this context.

VI. Acknowledgement

This work was funded by the Italian Ministry of Education, University and Research (MIUR) within the framework of the PRIN 2017-WPT4WID ("Wireless Power Transfer for Wearable and Implantable Devices") project.

References

[1] S. Li, T. Chi, Y. Wang, and H. Wang, "A millimeter-wave dual-feed square loop antenna for 5g communications," *IEEE Transactions on Antennas and Propagation*, vol. 65, no. 12, pp. 6317–6328, 2017.

[2] M. Wagih, L. Balocchi, F. Benassi, N. B. Carvalho, J.-C. Chiao, R. Correia, A. Costanzo, Y. Cui, D. Georgiadou, C. Gouveia, J. Grosinger, J. S. Ho, K. Hu, A. Komolafe, S. Lemey, C. Loss, G. Marrocco, P. Mitcheson, V. Palazzi, N. Panunzio, G. Paolini, P. Pinho, J. Preishuber-Pflgl, Y. Qaragoez, H. Rahmani, H. Rogier, J. R. Lopera, L. Roselli, D. Schreurs, M. Tentzeris, X. Tian, R. Torah, R. Torres, P. Van Torre, D. Vital, and S. Beeby, "Microwave-enabled wearables: Underpinning technologies, integration platforms, and next-generation roadmap," *IEEE Journal of Microwaves*, vol. 3, no. 1, pp. 193–226, 2023.

[3] M. Nariman, F. Shirinfar, A. Papi Toda, S. Pamarti, A. Rofougaran, and F. De Flaviis, "A compact 60-ghz wireless power transfer system," *IEEE Transactions on Microwave Theory and Techniques*, vol. 64, no. 8, pp. 2664–2677, 2016.

[4] E. Negri, F. Benassi, W. Fuscaldo, D. Masotti, P. Burghignoli, A. Costanzo, and A. Galli, "Effective te-polarized bessel-beam excitation for wireless power transfer near-field links," in *2022 52nd European Microwave Conference (EuMC)*, 2022, pp. 230–233.

[5] M. Ettorre and A. Grbic, "Generation of propagating bessel beams using leaky-wave modes," *IEEE Transactions on Antennas and Propagation*, vol. 60, no. 8, pp. 3605–3613, 2012.

[6] D. Masotti, A. Costanzo, M. Del Prete, and V. Rizzoli, "Time-modulation of linear arrays for real-time reconfigurable wireless power transmission," *IEEE Transactions on Microwave Theory and Techniques*, vol. 64, no. 2, pp. 331–342, 2016.

[7] Z. N. Chen, C. K. Goh, and X. Qing, "Loop antenna for uhf near-field rfid reader," in *Proceedings of the Fourth European Conference on Antennas and Propagation*. IEEE, 2010, pp. 1–4.

[8] V. Rizzoli, D. Masotti, N. Arbizzani, and A. Costanzo, "Cad procedure for predicting the energy received by wireless scavenging systems in the near-and far-field regions," in *2010 IEEE MTT-S International Microwave Symposium*. IEEE, 2010, pp. 1768–1771.

[9] Q. W. Lin and X. Y. Zhang, "Differential rectifier using resistance compression network for improving efficiency over extended input power range," *IEEE Transactions on Microwave Theory and Techniques*, vol. 64, no. 9, pp. 2943–2954, 2016.

[10] M.-D. Wei, Y.-T. Chang, D. Wang, C.-H. Tseng, and R. Negra, "Balanced rf rectifier for energy recovery with minimized input impedance variation," *IEEE Transactions on Microwave Theory and Techniques*, vol. 65, no. 5, pp. 1598–1604, 2017.

[11] P. Wei, W. Che, Z. Bi, C. Wei, Y. Na, L. Qiang, and M. Hao, "High-efficiency differential rf front-end for a gen2 rfid tag," *IEEE Transactions on Circuits and Systems II: Express Briefs*, vol. 58, no. 4, pp. 189–194, 2011.

[12] M. M. Mansour, X. Le Polozec, and H. Kanaya, "Compact and wide-band efficiency improved rf differential rectifier for wireless energy harvesting," in *2018 IEEE/MTT-S International Microwave Symposium-IMS*. IEEE, 2018, pp. 972–975.

[13] I. Adam, M. Fareq Abd Malek, M. Najib Mohd Yasin, and H. A. Rahim, "Double band microwave rectifier for energy harvesting," *Microwave and Optical Technology Letters*, vol. 58, no. 4, pp. 922–927, 2016.

[14] H. Takhedmit, B. Merabet, L. Cirio, B. Allard, F. Costa, C. Vollaire, and O. Picon, "Design of a 2.45 ghz rectenna using a global analysis technique," in *2009 3rd European Conference on Antennas and Propagation*. IEEE, 2009, pp. 2321–2325.

[15] M. Goldfarb and R. Pucel, "Modeling via hole grounds in microstrip," *IEEE Microwave and Guided Wave Letters*, vol. 1, no. 6, pp. 135–137, 1991.